An in-situ record of major environmental transitions on early Mars at Northeast Syrtis Major

Bethany L. Ehlmann[1,2] and John F. Mustard[3]

Received 3 March 2012; revised 6 May 2012; accepted 8 May 2012; published 6 June 2012.

[1] The Noachian-Hesperian transition on Mars was a period marked by changes in volcanic processes and styles of aqueous alteration. Understanding the timing and nature of environmental change requires the exploration of units recording both sets of processes. Herein, we report the compositional stratigraphy of distinctive Noachian to Hesperian units along the northeastern margin of the Syrtis Major volcanic flows. A layered, polyhydrated sulfate-bearing unit with jarosite ridges has been discovered beneath the Syrtis Major lava flows and above the regionally-extensive stratigraphy of Noachian plains units reported previously. Sequential clay-, carbonate-, and sulfate-bearing units formed in-situ and record a transition from alkaline pH to acidic pH waters. The sequence is chronologically bookended by the Isidis impact and Syrtis Major flows, and is one of the most temporally-constrained and well-preserved stratigraphic sections from early Mars available for landed exploration.
Citation: Ehlmann, B. L., and J. F. Mustard (2012), An in-situ record of major environmental transitions on early Mars at Northeast Syrtis Major, *Geophys. Res. Lett.*, *39*, L11202, doi:10.1029/2012GL051594.

1. Introduction

[2] The transition between the Noachian and Hesperian epochs on Mars is marked by evidence for a fundamental change in planetary-scale processes. Large volcanic provinces were emplaced broadly across Mars including the northern plains, Hesperia Planum and Syrtis Major [*Greeley and Spudis*, 1981; *Head et al.*, 2002; *Hiesinger and Head*, 2004]. Morphologic data suggest enhanced activity in valley networks [*Howard et al.*, 2005; *Irwin et al.*, 2005; *Fassett and Head*, 2008]. Mineralogic data suggest a transition from phyllosilicate formation and circum-neutral pH aqueous processes to a more acidic, water-limited sulfate-forming era [*Bibring et al.*, 2006]. Key to discerning the nature and causes of observed environmental transitions on early Mars is the discovery and characterization of continuous stratigraphic sections with rock units that span this time interval. Moreover, these sections are targets of interest for future in-situ exploration and sample return. Sites with well-constrained ages, ordered stratigraphies, and both primary igneous products as well as diverse alteration minerals formed in aqueous, potentially habitable environments are of highest interest. We detail the stratigraphic section preserved at Northeast Syrtis with particular emphasis on the new discovery of sulfate minerals and evidence for changing aqueous environments.

2. Study Area and Methods

[3] The ~1900 km diameter Isidis basin was emplaced in the early to middle Noachian between 3.85 and 4.06 billion years ago [*Schultz and Frey*, 1990; *Nimmo and Tanaka*, 2005; *Werner*, 2008]. To the west of the basin, in dissected and cratered Noachian plains units, are graben concentric to Isidis, known as the Nili Fossae [*Greeley and Guest*, 1987]. Within the Noachian plains, high-resolution spectroscopy and imaging reveal two extensive units: an upper olivine-rich unit [*Hoefen et al.*, 2003; *Hamilton and Christensen*, 2005] overlying a basement unit enriched in low-calcium pyroxene [*Mustard et al.*, 2007, 2009]. The regional olivine-unit is hypothesized to represent post-Isidis lava flows [*Hamilton and Christensen*, 2005; *Tornabene et al.*, 2008] or cumulates from the Isidis melt sheet [*Mustard et al.*, 2007, 2009]. Lavas of the high-calcium pyroxene-bearing Syrtis Major volcanic complex, emplaced during the early Hesperian, cover the southern exposure of the Noachian plains [*Hiesinger and Head*, 2004; *Werner*, 2009; *Mustard et al.*, 2005] (Figure 1).

[4] Both mineralogic and morphologic evidence indicate regional aqueous activity spanning a long time interval. In the lowermost exposed units, low-calcium pyroxene-enriched lithologies are intermixed with clay-bearing units exhibiting both brecciated and sedimentary textures [*Mangold et al.*, 2007; *Mustard et al.*, 2007, 2009]. The olivine-bearing unit is variably altered to Mg-carbonate [*Ehlmann et al.*, 2008a, 2009] and, less commonly, serpentine [*Ehlmann et al.*, 2010]. Valley networks and amphitheatre-headed valleys are found throughout the region [*Mangold et al.*, 2007], and sedimentary deposits contain Fe/Mg smectite clays and occasionally carbonates [*Ehlmann et al.*, 2008b, 2009]. The largest valley system, feeding the Jezero crater, was active in the late Noachian [*Fassett and Head*, 2005]. Smaller outflow channels superimposed on the Syrtis Major formation testify to episodic groundwater discharge following the end of volcanic activity in the Hesperian [*Mangold et al.*, 2008] (Figure 1).

[1]Division of Geological and Planetary Sciences, California Institute of Technology, Pasadena, California, USA.
[2]Jet Propulsion Laboratory, California Institute of Technology, Pasadena, California, USA.
[3]Department of Geological Sciences, Brown University, Providence, Rhode Island, USA.

Corresponding author: B. L. Ehlmann, Division of Geological and Planetary Sciences, California Institute of Technology, MC 170-25, 1200 E. California Blvd., Pasadena, CA 91125, USA. (ehlmann@caltech.edu)

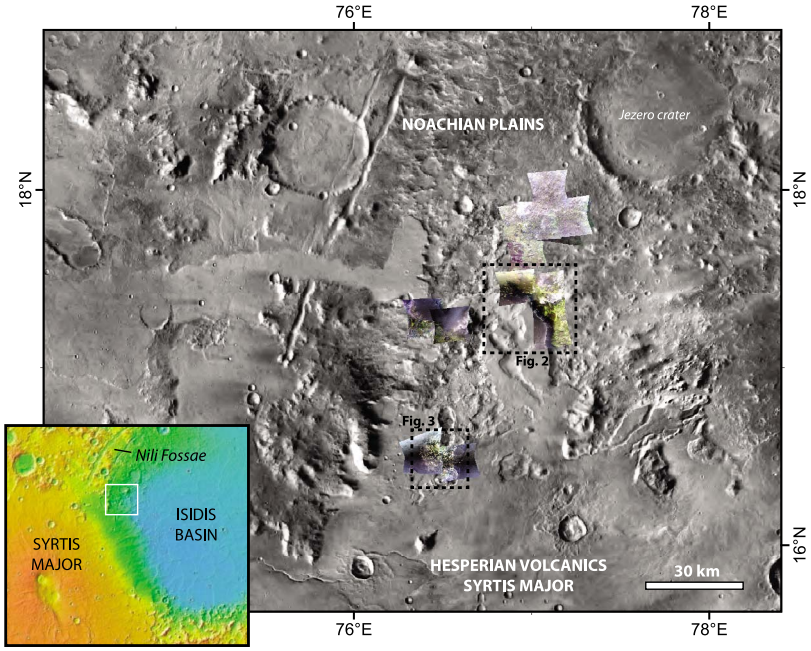

Figure 1. NE Syrtis region. Lavas of the early Hesperian Syrtis Major formation overlie Noachian terrains south of the Nili Fossae. The boundary between the two units is eroded and irregular. Channels and valleys formed during dissection by fluvial activity, which both pre-dates and post-dates lava emplacement. Targeted CRISM false-color images (red: 2.38 μm, green: 1.80 μm, blue: 1.15 μm) are overlain on a THEMIS daytime infrared image. In this color combination, mafic lavas (relatively flat spectrally) are purple, a carbonate-olivine unit green, sulfates white, and smectite clay minerals cyan to white. The inset for regional context is MOLA topography on a hillshade map and NE Syrtis is indicated by the white box.

The highly irregular margins of the lava flows have been hypothesized to result from the interaction of lavas with an ice-rich unit [*Ivanov and Head*, 2003].

[5] To refine the timing and nature of geologic processes, with particular focus on aqueous activity, we have examined the NE Syrtis region using new high-resolution image data collected from the Mars Reconnaissance Orbiter. Targeted data (18–40 m/pixel; 0.4–4 μm) from the Compact Reconnaissance Imaging Spectrometer for Mars (CRISM) [*Murchie et al.*, 2009] were photometrically and atmospherically corrected (for processing steps, see *Mustard et al.* [2008] and *Ehlmann et al.* [2009]) and have been used to identify and map the mafic and hydrous minerals in the region. These maps have been co-registered with high-resolution imaging data from the HiRISE and CTX cameras to distinguish geologic units on the basis of mineralogy and morphology [*McEwen et al.*, 2007; *Malin et al.*, 2007]. Stereo CTX anaglyphs along with MOLA topographic data have been used to identify contacts between units and estimate thicknesses to construct a stratigraphy spanning the early-Noachian to Hesperian.

3. The Sulfate-Bearing Unit

[6] New MRO-CRISM data reveal sulfate-bearing materials in multiple locations directly beneath the Syrtis Major surface (Figure 2). An asymmetric doublet centered at 2.21 μm and 2.26 μm results from Fe-OH absorptions in jarosite ($(Na,K,H_3O)Fe^{3+}{}_3OH)_6(SO_4)_2$ [*Swayze et al.*, 2008]). Though nominally anhydrous, jarosite spectra here possess 1.4-μm and 1.9-μm absorptions, indicating the presence of H_2O and that the jarosite may be in a mixture with other hydrated phases. Within the same stratigraphic unit, adjacent, similar materials have absorptions at 1.4 μm and 1.9 μm and an inflection at 2.4 μm, all of which are due to H_2O in the mineral structure. Because of the association with jarosite, we infer that these materials contain polyhydrated sulfates (e.g., $(Na_2,Ca,Mg)SO_4{\cdot}nH_2O$), although other hydrated salts and zeolites cannot be excluded on the basis of the spectral data.

[7] The morphologic character of the sulfate unit varies depending on the location. It is relatively brighter than the overlying Syrtis Major materials and consists of quasi-planar layers, sometimes contiguous over up to 1 km (Figure 2). In places, a distinctive box-work structure is exposed where raised ridges cross nearly orthogonally and cut the layered materials (Figure 2d). The jarosite absorption features are strongest within the high-standing bright materials while polyhydrated sulfates with only slight absorptions due to a jarosite component are within the layered deposits (Figure 3). The full extent of the sulfate-bearing deposits is still being mapped via acquisition of additional MRO data, but the sulfate-bearing units are found both at the scarp and in an erosional window beneath the Syrtis Major lavas over 60 km away (Figure 1). If contiguous, this implies a unit over a thousand square kilometers in areal extent.

4. NE Syrtis Stratigraphy

[8] The sulfates lie within a regionally extensive sequence of four stratigraphic units, from uppermost to lowest: (1) the early Hesperian Syrtis Major lavas, (2) the layered sulfates, (3) an olivine-enriched unit variably altered to carbonate and serpentine, and (4) an early Noachian, Fe/Mg smectite- and low-calcium pyroxene-bearing unit variably altered to Al-

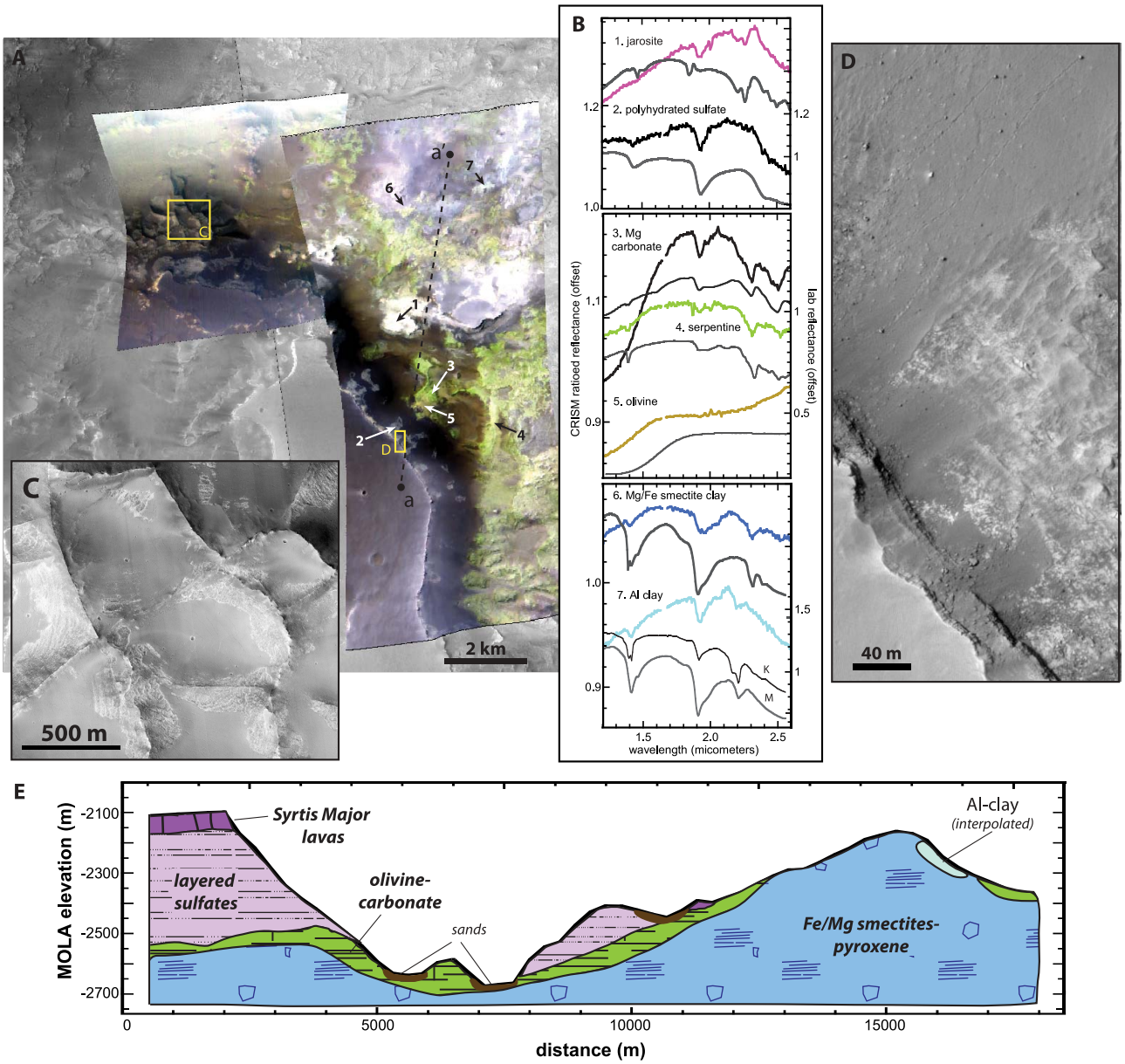

Figure 2. Sulfates exposed near the NE Syrtis scarp. (a) False-color CRISM images (HRL0000B8C2, FRT000128D0) at the northern extent of the Syrtis Major lava flows (purple in Figure 2a) are overlain on CTX images. (b) Sulfates (bright white in Figure 2a), including jarosite and a polyhydrated phase, are identified in B8C2 by comparison to laboratory data and overlie a Noachian olivine-rich unit (green in Figure 2a), which has been variably altered to Mg carbonate and serpentine [*Ehlmann et al.*, 2008a, 2010]. This in turn overlies a basement unit with Mg-rich smectites and Al-clays (cyan to white in Figure 2a). (c) In some locations, sulfate-bearing materials exhibit a ridged, box-like structure upon erosion, interpreted to represent exhumed, mineralized conduits of subsurface fluids (subset of ESP_013041_1975). (d) A tens-of-meter-thick, coherent Syrtis Major lava unit that sheds boulders overlies the sulfate-bearing unit. Boulder trails are visible at upper left in this subset of HiRISE PSP_009217_1975. (e) MOLA point shot data profile a-a′ shows contacts between the stratigraphic units are unconformable with superposition of later units on pre-existing topography.

clay-bearing materials (Figure 2b). The Syrtis Major lavas are layered, cliff-forming and shed boulders onto the more gently sloped sulfate-bearing materials beneath (Figure 2e). Lava thickness is approximately 45 m and angle of the cliff face is 55° based on photoclinometry using HiRISE data. The sulfates are thicker and are exposed over ~1 km lateral distance along an erosional face at the flow margin. MOLA point shot data and gridded products acquired in the region provide a means of assessing sulfate unit thickness: ~250–300 m with a modest slope of ~15–20° for the exposure near Figure 2.

[9] As noted previously for terrains to the north [*Mustard et al.*, 2009], the olivine-bearing unit conforms to the underlying basement topography. Near the lava scarp face (B8C2), the olivine-bearing unit is relatively flat lying, although the overall elevation range spanned by the olivine unit within CRISM image HRL0000B8C2 is 600 m, MOLA point shot data on and off outcrops show unit thicknesses

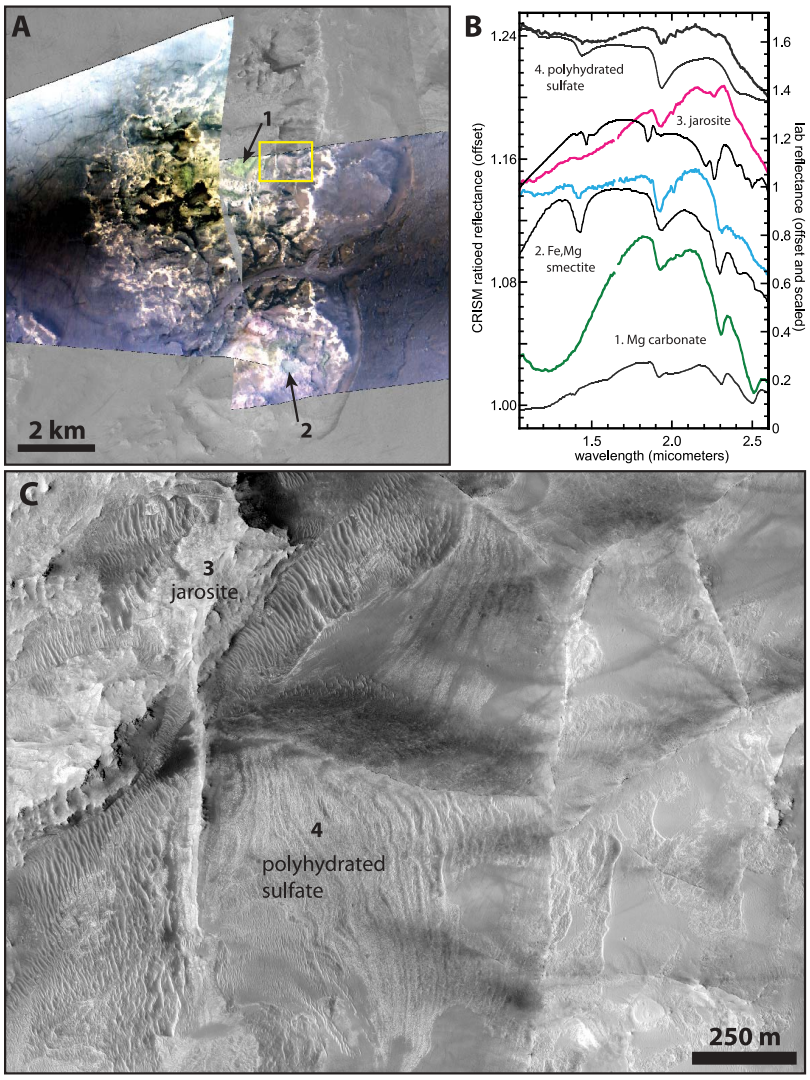

Figure 3. Erosional window within the Syrtis Major lavas. (a) False-color CRISM images (FRT000048B2, FRT0000821F) over a CTX image (P13_006000_1974_XI_17N283W_071106) show diverse compositions in the exposed terrains underlying and embayed by the Syrtis lavas. (b) Alteration minerals identified in 48B2 include magnesium carbonate (green), Fe, Mg smectite (cyan), and sulfate-bearing materials with compositions spectrally dominated by jarosite (magenta spectrum) and polyhydrated sulfate (black spectrum). (c) The bright-toned sulfate-bearing materials (yellow box in Figure 3a; subset of subset of HiRise PSP_006000_1965) have distinctive morphology, coupled to mineralogy. Jarosite detections preferentially occur in raised ridges while the polyhydrated sulfates are in layered materials.

between 35 m and 160 m. A variable thickness unit is in agreement with earlier observations north in and around the Nili Fossae [*Mustard et al.*, 2009]. Banding or layering, a key characteristic of the olivine-carbonate unit to the north, is less apparent here. In contrast, evidence for aqueous alteration is more pronounced. Most of the olivine-bearing unit at NE Syrtis has the VNIR spectral signature of magnesium carbonate, with relatively "pure" olivine spectral properties restricted to nearby sand dunes.

[10] Finally, the basement terrains contain Al clays and Fe/Mg smectite clays with low-calcium pyroxene. While stratigraphically the lowest, these units are topographically the highest at both the flow boundary and within the erosional window. Hills with Fe/Mg smectites and pyroxene in Figures 2 and 3 are at a MOLA elevation of approximately −1900 m, while the sulfates are found at low elevations between −2550 m and −2250 m. Mg-rich smectites are indicated by absorption positions at 1.39 μm and 2.31 μm. The clay-bearing units are partially obscured by shedding debris, but short, linear ridges are present within otherwise homogenous deposits [*Saper and Mustard*, 2012]. Brighter Al clay-bearing materials are above the Fe/Mg smectites and found in small patches of less than a kilometer in extent within the basement, a relationship that is also typical further north [*Ehlmann et al.*, 2009]. Kaolinite is the typical Al clay mineral elsewhere in the region; here, an Al-smectite clay or mixture of Al clays matches the spectral properties of the material (Figure 2b).

5. Discussion

5.1. Local History of Environmental Change

[11] The mismatch between stratigraphic and topographic ordering defies a simple characterization of either

sedimentary, weathering, or igneous processes, pointing rather to multiple cycles of deposition and erosion by multiple processes recorded at NE Syrtis. Based on the work at this site and previous studies of the region (reviewed in section 2), a sequence of events spanning the early Noachian to early Hesperian can be discerned, as follows. (1) Low-calcium pyroxene-bearing igneous bedrock is formed in the early Noachian, and subsequently partially aqueously altered to Fe/Mg smectite. (2) This bedrock is disrupted by the Isidis-forming impact, leading to breccias in some locations. (3) An olivine-rich unit is emplaced either as cumulates from an impact melt sheet or as fluid, post-impact lavas, which drape preexisting topography. (4) Substantial erosion, including by fluvial valley networks, carves channels, deposits clay- and carbonate-bearing sediments in Jezero crater and other topographic lows. Enhanced near-surface aqueous activity also leads to alteration of the olivine-rich unit to magnesium carbonate and the smectite-pyroxene unit to aluminous clays. (5) The sulfate-bearing materials are deposited on top of the olivine-carbonate unit, filling in topographic lows. (6) Syrtis Major volcanics then overtop these materials. The emplacement of the capping Syrtis Major lavas signals the end of aqueous activity in the region sufficient to be recorded by well-crystalline alteration minerals, although interaction with atmospheric volatiles [*Skok et al.*, 2010] and catastrophic floods [*Mangold et al.*, 2008] may have continued to modify the Syrtis Major lavas and other exposed surfaces until the Amazonian.

5.2. Sulfates, an Acidic Environment: Weathering, Lacustrine, or Hydrothermal?

[12] In contrast to the neutral to alkaline pH waters implied by the presence of Fe/Mg clays, magnesium carbonate, and serpentine in the older, lower stratigraphic units [*Ehlmann et al.*, 2008a, 2009, 2010], acidic conditions prevailed during formation of the sulfate deposits at NE Syrtis. Polyhydrated sulfates are a sufficiently diverse group that they do not serve as markers for specific aqueous geochemical conditions, but the presence of jarosite implies highly oxidizing and acidic (pH < 4) conditions [*Papike et al.*, 2006]. As is the case for the jarosite discovered from orbit around Valles Marineris [*Milliken et al.*, 2008] and at Mawrth Vallis [*Farrand et al.*, 2009], the NE Syrtis data include H_2O-related absorption features. These are consistent with an H_3O-bearing, Fe-deficient jarosite that forms via precipitation from relatively low temperature waters [*Swayze et al.*, 2008]. However, an alternative explanation for the observed spectral properties is a hydrothermal Na- or K-jarosite in a mineral assemblage with other species that can contain H_2O such as silica, kaolin family minerals, and other sulfates.

[13] We infer that the jarosite-enriched boxwork structures, i.e., raised ridges in the sulfates, are exposed, mineralized fractures, now topographically higher due to erosion of weaker surrounding materials. Fluid-altered fractures, similar to the high-standing components of the sulfates at NE Syrtis, have been reported in the layered sulfates at Valles Marineris [*Okubo and McEwen*, 2007]. Regardless of whether the layering process at NE Syrtis was volcanic or sedimentary, these mineralized ridges indicate that there has been a post-depositional episode, involving migration of subsurface fluids along fractures and the precipitation of jarosite-bearing materials.

[14] On Earth, jarosite forms in a variety of settings including via atmospheric oxidative weathering of pyrite, precipitation from acid sulfate lakes, and by oxidation of H_2S in volcanic hydrothermal environments. A scenario solely involving weathering is less likely here due to homogeneity over the 1 km thickness of the deposits and lack of pyrite identification (to date) in any Martian volcanics. Two end-member scenarios for the formation of the layered sulfates at NE Syrtis are volcanic-hydrothermal and lacustrine-groundwater. In the volcanic-hydrothermal scenario, the layered materials are igneous, i.e., the layering results from successive lava flows or ash deposits. Following and/or concurrent with lava emplacement, surface-derived or subsurface fluids with acidity derived from sulfurous volcanic gases circulate extensively through the fractured lava flows, leading to alteration and precipitation of sulfates, with higher jarosite concentrations in fractures. Only the last flows, the upper 45 m of Syrtis Major lavas, escape being part of this large regional hydrothermal system, comparable to modern-day sulfurous alteration of Icelandic lavas [*Kaasalainen and Stefansson*, 2011] or acid sulfate environments at the Hawaiian volcanoes [*Swayze et al.*, 2002].

[15] In the lacustrine-groundwater hypothesis, the layered materials are deposited as evaporite sediments, similar to sulfate formation in playa and dune settings at Meridiani Planum [*McLennan et al.*, 2005] or in the crater lake basins of Terra Sirenum [*Wray et al.*, 2011]. Subsequent acidic fluid flow and diagenesis lead to concentrations of jarosite in fracture systems. The fluid flow may have been local expression of an extensive groundwater aquifer system [*Andrews-Hanna and Lewis*, 2011] or may have been driven by release of volatiles and contact metamorphism of the underlying sediments by emplacement of hot Syrtis lavas [*Harvey and Griswold*, 2010] above a volatile-bearing unit [*Ivanov and Head*, 2003].

[16] Nighttime thermal infrared data from the sulfate-bearing units are intermediate between the Syrtis lava and olivine-carbonate units (high thermal inertia) and unconsolidated fines (low thermal inertia). Consequently, these data do not provide conclusive evidence for either scenario; both sediments and highly altered bedrock might have similar nighttime temperatures. Sedimentary bedforms have not been observed within the layered sulfates in images acquired to date. HiRISE stereo data to determine bed dip angles are not yet available but may provide insight on emplacement mechanisms.

5.3. Timing, Global Context, Future Exploration

[17] The clay-carbonate units west of Isidis had previously been somewhat unique, apparently preserving a record only of neutral to alkaline processes. In contrast, the stratigraphic sections at Mawrth Vallis, Meridiani Planum, and Valles Marineris capture evidence for acid-sulfate forming conditions. The discovery of sulfates at NE Syrtis extends the record of aqueous alteration in this region forward in time and also captures an apparently globally significant neutral/alkaline to acid geochemical transition. In contrast to the late Noachian to Amazonian stratigraphic section recorded in Gale crater sediments [*Milliken et al.*, 2010], the NE Syrtis section captures an older period, of impact bombardment, volcanism, and aqueous alteration from the early Noachian through the Hesperian. Furthermore, the NE Syrtis record is largely inferred to be one of in-situ alteration, rather than

deposition of transported materials. Alteration is partial, and both products and reactants are present in the units. Complete mineral assemblages or chemical data obtainable in-situ would enable calculations of the free energy of reactions and reconstruction of the environment(s) of aqueous alteration. A particularly interesting contact is that between the acid sulfates and carbonate: did acid fluids dissolve carbonate along an interface? How could the carbonates have persisted?

[18] Jarosite, first discovered at Meridiani Planum [*Klingelhöfer et al.*, 2004], is increasingly recognized in landed and orbital data as a characteristic of Hesperian and later alteration, found at Valles Marineris [*Milliken et al.*, 2008], Mawrth Vallis [*Farrand et al.*, 2009], and Terra Sirenum [*Wray et al.*, 2011]. Interestingly for future potential landed investigations at NE Syrtis, the different possible jarosite formation mechanisms, indistinguishable at orbital scale, are distinguishable using textural evidence at cm- to mm-scale and in S and O stable isotope data. The jarosite structure is remarkably tolerant of cation substitutions, is a robust chronometer for Ar-Ar and K-Ar dating, and may be a successful host for other stable isotopes useful in age dating [*Papike et al.*, 2006]. This, coupled with the defined lower (early Noachian) and upper (early Hesperian) ages at NE Syrtis, makes the site ideal for study of the timing and evolution of key planetary processes such as late-heavy bombardment, fluvial activity associated with valley network formation, groundwater circulation, and volcanic activity.

6. Conclusions

[19] The stratigraphy at NE Syrtis spans the early Noachian to early Hesperian, preserving a time-ordered record of basin-forming impacts, fluvial activity, aqueous alteration, plains volcanism, and catastrophic outflow channels. The variable primary mineralogy (olivine, low- and high-calcium pyroxene) in strata of different units records a change in the nature of igneous processes, and the mineralogy of alteration minerals records a change in water chemistry from neutral to alkaline pH conditions promoting clay and carbonate formation to highly acidic conditions promoting formation of jarosite in fluidized fractures within layered sulfate-bearing deposits. These well-preserved strata present an opportunity for testing key hypotheses regarding geologic processes and environmental change on early Mars and provide a diversity of stratigraphic units for return of Martian samples to Earth.

[20] **Acknowledgments.** The authors thank R. Harvey for initial discussions about the timing of processes related to volcanic emplacement and J.R. Skok for discussions on stratigraphy.

[21] The Editor thanks Harold Clenet and an anonymous reviewer for assisting in the evaluation of this paper.

References

Andrews-Hanna, J. C., and K. W. Lewis (2011), Early Mars hydrology: 2. Hydrological evolution in the Noachian and Hesperian epochs, *J. Geophys. Res.*, *116*, E02007, doi:10.1029/2010JE003709.

Bibring, J.-P., et al. (2006), Global mineralogical and aqueous Mars history derived from OMEGA/Mars Express data, *Science*, *312*, 400–404, doi:10.1126/science.1122659.

Ehlmann, B. L., et al. (2008a), Orbital identification of carbonate-bearing rocks on Mars, *Science*, *322*, 1828–1832, doi:10.1126/science.1164759.

Ehlmann, B. L., et al. (2008b), Clay-bearing minerals and organic preservation potential in sediments from a Martian delta environment, Jezero crater, Nili Fossae, Mars, *Nat. Geosci.*, *1*, 355–358, doi:10.1038/ngeo207.

Ehlmann, B. L., et al. (2009), Identification of hydrated silicate minerals on Mars using MRO-CRISM: Geologic context near Nili Fossae and implications for aqueous alteration, *J. Geophys. Res.*, *114*, E00D08, doi:10.1029/2009JE003339.

Ehlmann, B. L., J. F. Mustard, and S. L. Murchie (2010), Geologic setting of serpentine deposits on Mars, *Geophys. Res. Lett.*, *37*, L06201, doi:10.1029/2010GL042596.

Farrand, W. H., et al. (2009), Discovery of jarosite within the Mawrth Vallis region of Mars: Implications for the geologic history of the region, *Icarus*, *204*, 478–488, doi:10.1016/j.icarus.2009.07.014.

Fassett, C. I., and J. W. Head III (2005), Fluvial sedimentary deposits on Mars: Ancient deltas in a crater lake in the Nili Fossae region, *Geophys. Res. Lett.*, *32*, L14201, doi:10.1029/2005GL023456.

Fassett, C. I., and J. W. Head III (2008), The timing of Martian valley network activity: Constraints from buffered crater counting, *Icarus*, *195*, 61–89, doi:10.1016/j.icarus.2007.12.009.

Greeley, R., and J. E. Guest (1987), Geologic map of the eastern equatorial region of Mars, *U.S. Geol. Surv. Misc. Invest. Ser. Map*, *I-1802-B*.

Greeley, R., and P. Spudis (1981), Volcanism on Mars, *Rev. Geophys.*, *19*(1), 13–41, doi:10.1029/RG019i001p00013.

Hamilton, V. E., and P. R. Christensen (2005), Evidence for extensive, olivine-rich bedrock on Mars, *Geology*, *33*, 433–436, doi:10.1130/G21258.1.

Harvey, R. P., and J. Griswold (2010), Burial, exhumation, metamorphism and other dastardly deeds exposed at the Hesperian/Noachian boundary in the southern Nili Fossae region, *Lunar Planet. Sci. Conf.*, *41st*, Abstract 2045.

Head, J. W., III, M. A. Kreslavsky, and S. Pratt (2002), Northern lowlands of Mars: Evidence for widespread volcanic flooding and tectonic deformation in the Hesperian Period, *J. Geophys. Res.*, *107*(E1), 5003, doi:10.1029/2000JE001445.

Hiesinger, H., and J. W. Head (2004), The Syrtis Major volcanic province, Mars: Synthesis from Mars Global Surveyor data, *J. Geophys. Res.*, *109*, E01004, doi:10.1029/2003JE002143.

Hoefen, T. M., R. N. Clark, J. L. Bandfield, M. D. Smith, J. C. Pearl, and P. R. Christensen (2003), Discovery of olivine in the Nili Fossae region of Mars, *Science*, *302*, 627–630, doi:10.1126/science.1089647.

Howard, A. D., J. M. Moore, and R. P. Irwin (2005), An intense terminal epoch of widespread fluvial activity on early Mars: 1. Valley network incision and associated deposits, *J. Geophys. Res.*, *110*, E12S14, doi:10.1029/2005JE002459.

Irwin, R. P., III, et al. (2005), An intense terminal epoch of widespread fluvial activity on early Mars: 2. Increased runoff and paleolake development, *J. Geophys. Res.*, *110*, E12S15, doi:10.1029/2005JE002460.

Ivanov, M. A., and J. W. Head III (2003), Syrtis Major and Isidis Basin contact: Morphological and topographic characteristics of Syrtis Major lava flows and materials of the Vastitas Borealis Formation, *J. Geophys. Res.*, *108*(E6), 5063, doi:10.1029/2002JE001994.

Kaasalainen, H., and A. Stefansson (2011), Sulfur speciation in natural hydrothermal waters, Iceland, *Geochim. Cosmochim. Acta*, *75*, 2777–2791, doi:10.1016/j.gca.2011.02.036.

Klingelhöfer, G., et al. (2004), Jarosite and hematite at Meridiani Planum from Opportunity's Mössbauer spectrometer, *Science*, *306*, 1740–1745, doi:10.1126/science.1104653.

Malin, M. C., et al. (2007), Context Camera investigation on board the Mars Reconnaissance Orbiter, *J. Geophys. Res.*, *112*, E05S04, doi:10.1029/2006JE002808.

Mangold, N., et al. (2007), Mineralogy of the Nili Fossae region with OMEGA/Mars Express data: 2. Aqueous alteration of the crust, *J. Geophys. Res.*, *112*, E08S04, doi:10.1029/2006JE002835.

Mangold, N., V. Ansan, D. Baratoux, F. Costard, L. Dupeyrat, H. Hiesinger, P. Masson, G. Neukum, and P. Pinet (2008), Identification of a new outflow channel on Mars in Syrtis Major Planum using HRSC/MEx data, *Planet. Space Sci.*, *56*(7), 1030–1042, doi:10.1016/j.pss.2008.01.011.

McEwen, A. S., et al. (2007), Mars Reconnaissance Orbiter's High Resolution Imaging Science Experiment (HiRISE), *J. Geophys. Res.*, *112*, E05S02, doi:10.1029/2005JE002605.

McLennan, S. M., et al. (2005), Provenance and diagenesis of the evaporite-bearing Burns formation, Meridiani Planum, Mars, *Earth Planet. Sci. Lett.*, *240*, 95–121, doi:10.1016/j.epsl.2005.09.041.

Milliken, R. E., et al. (2008), Opaline silica in young deposits on Mars, *Geology*, *36*, 847–850, doi:10.1130/G24967A.1.

Milliken, R. E., J. P. Grotzinger, and B. J. Thomson (2010), Paleoclimate of Mars as captured by the stratigraphic record in Gale Crater, *Geophys. Res. Lett.*, *37*, L04201, doi:10.1029/2009GL041870.

Murchie, S. L., et al. (2009), Compact Reconnaissance Imaging Spectrometer for Mars investigation and data set from the Mars Reconnaissance Orbiter's primary science phase, *J. Geophys. Res.*, *114*, E00D07, doi:10.1029/2009JE003344.

Mustard, J. F., et al. (2005), Olivine and pyrorene diversity in the crust of Mars, *Science*, *307*, 1594–1597, doi:10.1126/science.1109098.

Mustard, J. F., F. Poulet, J. W. Head, N. Mangold, J.-P. Bibring, S. M. Pelkey, C. I. Fassett, Y. Langevin, and G. Neukum (2007), Mineralogy of the Nili Fossae region with OMEGA/Mars Express data: 1. Ancient

impact melt in the Isidis basin and implications for the transition from the Noachian to Hesperian, *J. Geophys. Res.*, *112*, E08S03, doi:10.1029/2006JE002834.

Mustard, J. F., et al. (2008), Hydrated silicate minerals on Mars observed by the CRISM instrument on MRO, *Nature*, *454*, 305–309, doi:10.1038/nature07097.

Mustard, J. F., B. L. Ehlmann, S. L. Murchie, F. Poulet, N. Mangold, J. W. Head, J.-P. Bibring, and L. H. Roach (2009), Composition, morphology, and stratigraphy of Noachian crust around the Isidis basin, *J. Geophys. Res.*, *114*, E00D12, doi:10.1029/2009JE003349.

Nimmo, F., and K. Tanaka (2005), Early crustal evolution of Mars, *Annu. Rev. Earth Planet. Sci.*, *33*, 133–161, doi:10.1146/annurev.earth.33.092203.122637.

Okubo, C. H., and A. S. McEwen (2007), Fracture-controlled paleo-fluid flow in Candor Chasma, Mars, *Science*, *315*, 983–985, doi:10.1126/science.1136855.

Papike, J. J., J. M. Karner, and C. K. Shearer (2006), Comparative planetary mineralogy: Implications of Martian and terrestrial jarosite. A crystal chemical perspective, *Geochim. Cosmochim. Acta*, *70*, 1309–1321, doi:10.1016/j.gca.2005.11.004.

Saper, L. M., and J. F. Mustard (2012), Orientations and morphology of linear ridges in Nili Fossae: Mineralized fracture zones and implications for crustal fluid transport, *Lunar Planet. Sci. Conf.*, *43rd*, Abstract 1119.

Schultz, R. A., and H. V. Frey (1990), A new survey of multiring impact basins on Mars, *J. Geophys. Res.*, *95*(B9), 14,175–14,189, doi:10.1029/JB095iB09p14175.

Skok, J. R., J. F. Mustard, S. L. Murchie, M. B. Wyatt, and B. L. Ehlmann (2010), Spectrally distinct ejecta in Syrtis Major, Mars: Evidence for environmental change at the Hesperian-Amazonian boundary, *J. Geophys. Res.*, *115*, E00D14, doi:10.1029/2009JE003338.

Swayze, G. A., et al. (2002), Mineral mapping Mauna Kea and Mauna Loa shield volcanoes on Hawaii using AVIRIS data and the USGS Tetracorder spectral identification system: Lessons applicable to the search for relict Martian hydrothermal systems, *JPL Publ.*, *03-4*, 373–387.

Swayze, G. A., G. A. Desborough, K. S. Smith, H. A. Lowers, J. M. Hammarstrom, S. F. Diehl, R. W. Leinz, and R. L. Driscoll (2008), Understanding jarosite—From mine waste to Mars, in *Understanding Contaminants Associated With Mineral Deposits*, edited by P. L. Verplanck, *U.S. Geol. Surv. Circ.*, *1328*, 8–13.

Tornabene, L. L., J. E. Moersch, H. Y. McSween Jr., V. E. Hamilton, J. L. Piatek, and P. R. Christensen (2008), Surface and crater-exposed lithologic units of the Isidis basin as mapped by coanalysis of THEMIS and TES derived data products, *J. Geophys. Res.*, *113*, E10001, doi:10.1029/2007JE002988.

Werner, S. C. (2008), The early Martian evolution—Constraints from basin formation ages, *Icarus*, *195*, 45–60, doi:10.1016/j.icarus.2007.12.008.

Werner, S. C. (2009), The global Martian volcanic evolutionary history, *Icarus*, *201*, 44–68, doi:10.1016/j.icarus.2008.12.019.

Wray, J. J., et al. (2011), Columbus crater and other possible groundwater-fed paleolakes of Terra Sirenum, Mars, *J. Geophys. Res.*, *116*, E01001, doi:10.1029/2010JE003694.